

# High-frequency surface acoustic wave propagation in nanostructures characterized by coherent extreme ultraviolet beams

Mark E. Siemens,<sup>1,a)</sup> Qing Li,<sup>1</sup> Margaret M. Murnane,<sup>1</sup> Henry C. Kapteyn,<sup>1</sup> Ronggui Yang,<sup>2</sup> Erik H. Anderson,<sup>3</sup> and Keith A. Nelson<sup>4</sup>

<sup>1</sup>Department of Physics and JILA, University of Colorado, Boulder, Colorado 80309-0440, USA

<sup>2</sup>Department of Mechanical Engineering, University of Colorado, Boulder, Colorado 80309-0440, USA

<sup>3</sup>Center for X-Ray Optics, Lawrence Berkeley National Laboratory, Berkeley, California 94720, USA

<sup>4</sup>Department of Chemistry, Massachusetts Institute of Technology, Cambridge, Massachusetts 02139, USA

(Received 30 January 2009; accepted 7 February 2009; published online 3 March 2009)

We study ultrahigh frequency surface acoustic wave propagation in nickel-on-sapphire nanostructures. The use of ultrafast, coherent, extreme ultraviolet beams allows us to extend optical measurements of propagation dynamics of surface acoustic waves to frequencies of nearly 50 GHz, corresponding to wavelengths as short as 125 nm. We repeat the measurement on a sequence of nanostructured samples to observe surface acoustic wave dispersion in a nanostructure series. These measurements are critical for accurate characterization of interfaces beneath very thin films using this technique. © 2009 American Institute of Physics. [DOI: 10.1063/1.3090032]

Monitoring surface acoustic wave (SAW) propagation is a powerful tool for studying the properties of thin films, surfaces, and interfaces. SAW modes have a very shallow surface penetration, and thus their propagation is sensitive to surface structure and composition. To study films of submicron thickness, however, it is necessary to use SAWs with comparably short wavelengths, since the penetration depth  $\zeta$  of the SAW is proportional to the acoustic wavelength  $\Lambda$  i.e.,  $\zeta = \Lambda/2\pi$ . This presents a challenge for conventional optical methods of creating and detecting SAWs. Although it is quite straightforward to manufacture a sub-100 nm thickness film, thermally exciting the film using a visible light interference pattern in a transient grating geometry is limited to SAW wavelengths in the range of optical wavelengths. As a result, the shortest acoustic wavelength generated to date using the transient grating method is approximately 750 nm.<sup>1,2</sup>

An alternative approach that overcomes this limitation is to pattern a nanostructure on the surface. This pattern can then be optically excited, locally stressing the surface, and thus exciting a SAW with a wavelength limited only by the resolution of the patterning technique.<sup>3,4</sup> However, this approach raises the question of how much the presence of the nanostructure will affect the propagation of the SAW. This question is critical for analysis of the underlying sample characteristics. Past measurements employing thin Al patterned absorbers suggested that these issues can be neglected.<sup>4-6</sup> However, these conclusions were based on data taken at a single SAW wavelength. To date, no work has sampled the full dispersion curve of a patterned thin film in order to come to a definitive conclusion.

Detection of very short-wavelength SAWs is also an issue. Visible light will not diffract from a subwavelength structure, so current techniques measure very small [ $<1$  part in  $10^5$  (Ref. 7)] changes in surface reflectivity to observe SAW propagation.<sup>4-6</sup> However, these reflectivity changes arise from a complex mix of induced density changes and local and interfacial stresses and strains. Direct transient grating diffraction from the surface would give more reliable

and easier-to-interpret data, however, such an experiment requires coherent light with a wavelength shorter than the SAW wavelength. For high acoustic frequencies, this corresponds to the extreme ultraviolet (EUV) region of the spectrum. In previous work, we demonstrated that coherent EUV beams can very sensitively probe acoustically induced surface displacements with subpicometer displacement resolution.<sup>8</sup> In that experiment, changes in the EUV diffraction were due to thermal and acoustic surface displacements, while temperature and stress-induced changes in reflectivity were negligible at the EUV wavelengths used ( $\sim 29$  nm).<sup>8</sup>

In this work, we excite a series of nickel-on-sapphire nanostructures, using a Ti:sapphire laser, to generate high-frequency acoustic waves. We study the SAW propagation in the nanostructures by observing the change in diffraction intensity of an EUV probe beam (see Fig. 1). We observe the highest-frequency SAW dynamics to date and demonstrate a measurement of SAW dispersion in these nanostructure/bulk systems. The acoustic wavelength is set by the nanostructure period and we find that for long acoustic wavelengths, the propagation of the SAW is dominated by the substrate properties. However, for shorter acoustic wavelengths, the penetration depth decreases and the SAW is increasingly localized in the nickel, slowing down the SAW propagation. Our

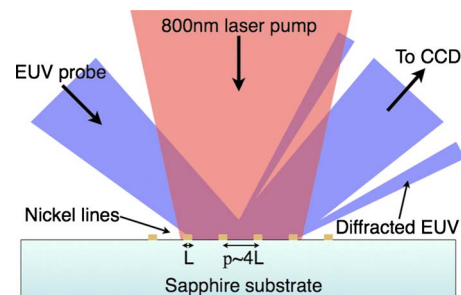


FIG. 1. (Color online) Setup for ultrafast SAW dispersion measurements. Nickel lines of thickness  $h=10$  or  $20$  nm, width  $L$  between  $65$  nm and  $2$   $\mu\text{m}$ , and period  $p$  are patterned on a sapphire substrate. An  $800$  nm laser pulse heats the Ni creating a periodic stress that excites a SAW. This SAW is then probed by observing the dynamically changing diffraction of an ultrafast  $29$  nm EUV pulse from the surface.

<sup>a)</sup>Electronic mail: siemens@colorado.edu.

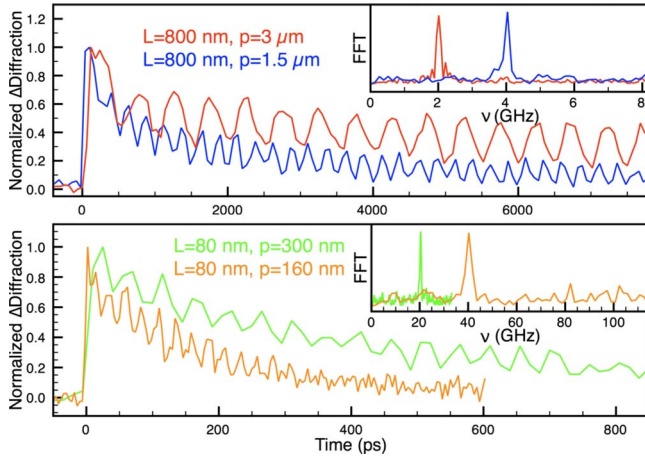


FIG. 2. (Color online) Dynamic EUV diffraction from SAWs on samples of sapphire with periodically spaced lines of nickel. Nickel line periods of  $p=1.5$  and  $3 \mu\text{m}$  with width of  $L=800 \text{ nm}$  (top) and  $p=300$  and  $160 \text{ nm}$  with  $L=80 \text{ nm}$  (bottom) were heated and probed. Impulsive heating and rapid thermal expansion launch SAWs whose oscillations are superimposed upon a nonoscillatory signal component that decays due to thermal diffusion. The SAW frequencies are shown in the insets.

data are in excellent agreement with an effective mass model for thin films, modified to account for the presence of the nanostructure.

The sample geometry is shown in Fig. 1. A laser heating beam and an EUV probe beam both originate from an ultrafast Ti:Sapphire laser-amplifier system generating  $2 \text{ mJ}$ ,  $25 \text{ fs}$  pulses at a wavelength of  $800 \text{ nm}$  and at a repetition rate of  $2 \text{ kHz}$ . The output of this laser is split into pump and probe beams. To generate the  $29 \text{ nm}$  probe beam, part of the  $800 \text{ nm}$  light is focused into a gas-filled hollow waveguide to generate high-order harmonics, which are then refocused onto the sample using a grazing-incidence toroidal mirror. The  $800 \text{ nm}$  pump beam is sent through a computer-controlled time-delay stage before being loosely focused onto the sample. A relatively large pump spot ( $\sim 700 \mu\text{m}$ ) is used so that the area probed will be uniformly heated with a fluence of  $2 \text{ mJ/cm}^2$ .

Sapphire was selected as the substrate material because it has a very high acoustic velocity (Rayleigh velocity  $v_{\text{Sa}} \sim 6300 \text{ m/s}$ ) and is transparent to the  $800 \text{ nm}$  pump light used for exciting the nanostructure. Nickel lines were manufactured using electron beam lithography and liftoff in  $120 \times 120 \mu\text{m}^2$  regions. Within each region, the lines were  $120 \mu\text{m}$  long with a fixed width  $L$  between  $65$  and  $2000 \text{ nm}$  (period confirmed by scanning electron microscopy). Two grating geometries were used: one with nickel strips of height  $h=20 \text{ nm}$  with period  $p=4L$ , the other with  $h=10 \text{ nm}$  and  $p=2L$ . Because the sapphire substrate is transparent to the  $800 \text{ nm}$  pump light, the pump pulse only heats the Ni nanostructure. The heat-induced periodic stress launches SAWs that travel along the surface perpendicular to the orientation of the nickel lines. These SAWs displace the nanostructure surface as they propagate. The small displacements are detected as changes in the diffraction efficiency of the probe EUV beam. By measuring the change in diffraction as a function of pump-probe delay time, we can observe the dynamic propagation of the SAW. Four scans with  $p=3 \mu\text{m}$ ,  $1.5 \mu\text{m}$ ,  $300 \text{ nm}$ , and  $160 \text{ nm}$  are shown in Fig. 2. The rise and subsequent decay in the signal are due to thermal expansion and subsequent dissipation of heat from the

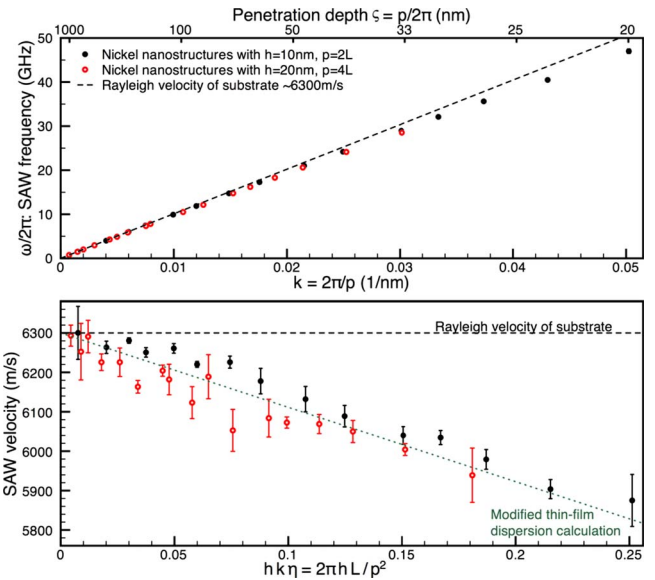


FIG. 3. (Color online) Measured SAW frequency (top) and velocity (bottom) for propagation in two sets of samples with nanopatterned Ni on sapphire. Significant deviation from the Rayleigh velocity in sapphire is observed for the smaller grating periods. The measured velocity dispersion agrees with an effective mass-loading calculation.

nanostructure into the substrate,<sup>9</sup> while the oscillation is due to SAW propagation. The relative amplitude of the SAW component of the signal is  $\sim 5\text{--}10\times$  larger than in a similar experiment using an optical probe.<sup>6</sup> For a given grating period  $p$ , we extract the SAW frequency  $\nu$  by performing a Fourier transform, as shown in the insets of Fig. 2.

Past work on acoustic dynamics in periodic nanostructures has focused on whether the observed signal is dominated by SAW propagation in the substrate or by normal mode resonances of individual wires.<sup>4,5,7</sup> To determine the relative contributions, we compared the results from the  $p=4L$  samples to those from  $p=2L$  samples, as shown in Fig. 2. For  $L=800 \text{ nm}$ , SAWs in the  $2L$  ( $p=1.5 \mu\text{m}$ ) sample have a frequency of  $4.01 \pm 0.01 \text{ GHz}$ , which is two times greater than the  $2.01 \pm 0.01 \text{ GHz}$  frequency in the  $4L$  ( $p=3 \mu\text{m}$ ) samples. The frequency of oscillation is proportional to the nickel strip period rather than the line width. We therefore conclude that the oscillation is due to SAW propagation in the substrate, with a SAW wavelength  $\Lambda$  set by the strip period ( $\Lambda=p$ ).

We repeat this measurement on samples with different nickel line widths to determine the dispersion curve of the SAW propagation in the Ni/sapphire nanostructure (Fig. 3). For long acoustic wavelengths (large  $p$ , small  $k$ ), the penetration depth is long, so the nanostructure can be ignored and the SAW velocity is the Rayleigh velocity in the sapphire substrate, i.e., frequency  $\nu = v_{\text{Sa}}/p$ , shown as a dashed line in Fig. 3. For shorter acoustic wavelengths, the penetration depth (see top  $x$ -axis in Fig. 3) is decreased and the SAW is increasingly localized in the nickel, slowing down the SAW propagation. Previous studies of Al/quartz (Ref. 5) and Al/Si (Ref. 6) structures at isolated acoustic wavelengths  $\Lambda > 200 \text{ nm}$  suggested that the SAW dispersion is minimal, but we observe significant SAW velocity dispersion at these wavelengths. The data show a small offset between the two different samples, which we attribute to small differences between the nominal and actual duty cycles. The  $\nu$

=47 GHz frequency of the  $p=125$  nm structure is the highest SAW frequency and shortest SAW wavelength measured optically.

A quantitative calculation of SAW propagation is complicated by the modified Brillouin zone, stop bands, and multimode propagation introduced by the nanostructure.<sup>10</sup> To first approximation, an effective mass model from thin film theory based on a perturbative expansion of the stress at the surface can be used.<sup>11</sup> Datta and Hunsinger<sup>12</sup> suggested an extension of this thin film theory to nanostructures, introducing a duty cycle factor  $\eta=L/p$  by which the dispersion effect is multiplied. Our data are in excellent agreement with this theory over the entire range of wavelengths (Fig. 3, bottom). These results will be useful in eliminating nanostructure-induced errors in similar measurements of thin film properties.

In conclusion, we used ultrafast coherent EUV pulses to measure ultrahigh-frequency SAW propagation and dispersion in nanostructures at frequencies up to  $\sim 50$  GHz. This technique of visible laser excitation and EUV probing can easily be extended to even shorter wavelengths (higher frequencies), limited only by lithographic capabilities. Thus, it holds promise for studying materials and interface properties of extremely thin films.

This work was supported by the Chemical Sciences, Geosciences, and Biosciences Division of the Office of Basic Energy Sciences, U.S. Department of Energy, Grant No. DE-FG02-00ER15087 and the NSF Engineering Research Center in EUV Science and Technology.

- <sup>1</sup>J. A. Rogers, L. Dhar, and K. A. Nelson, *Appl. Phys. Lett.* **65**, 312 (1994).
- <sup>2</sup>R. I. Tobey, M. E. Siemens, M. M. Murnane, H. C. Kapteyn, D. H. Torchinsky, and K. A. Nelson, *Appl. Phys. Lett.* **89**, 091108 (2006).
- <sup>3</sup>R. I. Tobey, E. H. Gershgoren, M. E. Siemens, M. M. Murnane, H. C. Kapteyn, T. Feurer, and K. A. Nelson, *Appl. Phys. Lett.* **85**, 564 (2004).
- <sup>4</sup>G. A. Antonelli, P. Zannitto, and H. J. Maris, *Physica B* **316**, 377 (2002).
- <sup>5</sup>B. Bonello, A. Ajinou, V. Richard, P. Djemia, and S. M. Cherif, *J. Acoust. Soc. Am.* **110**, 1943 (2001).
- <sup>6</sup>D. Hurley and K. Telschow, *Phys. Rev. B* **66**, 153301 (2002).
- <sup>7</sup>H.-N. Lin, H. J. Maris, L. B. Freund, K. Y. Lee, H. Luhn, and D. P. Kern, *J. Appl. Phys.* **73**, 37 (1993).
- <sup>8</sup>R. I. Tobey, M. E. Siemens, O. Cohen, M. M. Murnane, H. C. Kapteyn, and K. A. Nelson, *Opt. Lett.* **32**, 286 (2007).
- <sup>9</sup>M. Siemens, Q. Li, M. Murnane, H. Kapteyn, R. Yang, E. Anderson, and K. Nelson, "Measurement of quasi-ballistic thermal transport from nanoscale interfaces using ultrafast coherent soft x-ray beams," *Science* (submitted).
- <sup>10</sup>A. A. Maznev, *Phys. Rev. B* **78**, 155323 (2008).
- <sup>11</sup>B. A. Auld, *Acoustic Fields and Waves in Solids* (Wiley, New York, 1973), Vol. II, pp. 275–283 and 302–309.
- <sup>12</sup>S. Datta and B. J. Hunsinger, *J. Appl. Phys.* **50**, 5661 (1979).